The AMS-02 3D imaging calorimeter : a tool for cosmic rays in space

C. Goy

Laboratoire d'Annecy-le-Vieux
de Physique des Particules

LAPP-EXP-2008-01
September 2008

The AMS-02 3D-imaging calorimeter: a tool for cosmic rays in space

C. Goy
on behalf of the AMS Calorimeter Group

LAPP - Université de Savoie - IN2P3-CNRS
BP. 110, F-74941 Annecy-le-Vieux Cedex, France

Presented at the XIIIth International Conference on Calorimetry
in High Energy Physics, CALOR 2008
Pavia (Italy), 26-30 May 2008

CENTRE NATIONAL DE LA RECHERCHE SCIENTIFIQUE
IN2P3
INSTITUT NATIONAL DE PHYSIQUE NUCLÉAIRE ET DE PHYSIQUE DES PARTICULES
UNIVERSITE CHAMBERY ANNECY SAVOIE

The AMS-02 3D-imaging calorimeter: a tool for cosmic rays in space.

Corinne Goy LAPP, IN2P3/CNRS, Université de Savoie on behalf on the AMS calorimeter group.

Laboratoire d'Annecy-Le-Vieux de Physique des Particules, Chemin de Bellevue, F-74941 Annecy-Le-Vieux Cedex

E-mail: corinne.goy@lapp.in2p3.fr

Abstract. The AMS02 Electromagentic calorimeter (ECAL) is based on a lead/scintillating fiber sandwich. The flight model was tested and calibrated during Summer 2007 in a test beam at CERN, using 6 to 250 GeV electron and hadron beams. Preliminary results on the measurements of ECAL parameters and performances are reported in this paper.

1. Introduction

The AMS-02 experiment is a large acceptance spectrometer designed to operate on the International Space Station (ISS) for three years. The physics goals of the AMS experiment are:

- The measurement of the nature and fluxes of the cosmic rays up to the TeV range, including the identification of nuclei and light isotopes (^{3}He, B, C, ^{9}Be, ^{10}Be) and the galactic and extragalactic gamma rays spectra to a few 100 GeV.
- The search for an additional component originating from Dark Matter annihilations on top of the antiproton, positron or gamma spectra.
- The search for nuclear antimatter with an expected sensitivity of 10^{-9} for $\overline{\mathrm{He}}$/He and 10^{-7} for $\overline{\mathrm{C}}$/C.

The experimental setup (Figure 1) consists of a 8 layers silicon tracker inserted in a superconducting magnet providing a 0.8 Tm bending power. A total of 4 layers of Time Of Flight scintillating system situated on the top and the bottom of the tracker provides the main trigger and gives the direction of the particles. A set of Veto-Counters surrounds the tracker to reject side tracks. A Transition Radiator Detector and the calorimeter allow for electron, positron and gamma identification, while the Nuclei species are identified by the RICH detector in conjunction with the Tracker. The total acceptance amounts to 0.5 m^2.sr.

2. The calorimeter

The aim of the electromagnetic calorimeter is to measure the energy of electromagnetic particles from a few GeV up to 1 TeV, to produce a stand-alone gamma trigger, to give a rejection against hadrons with respect to electrons and positrons of the order 10^{-4} combined with the tracker, and to identify gamma rays.

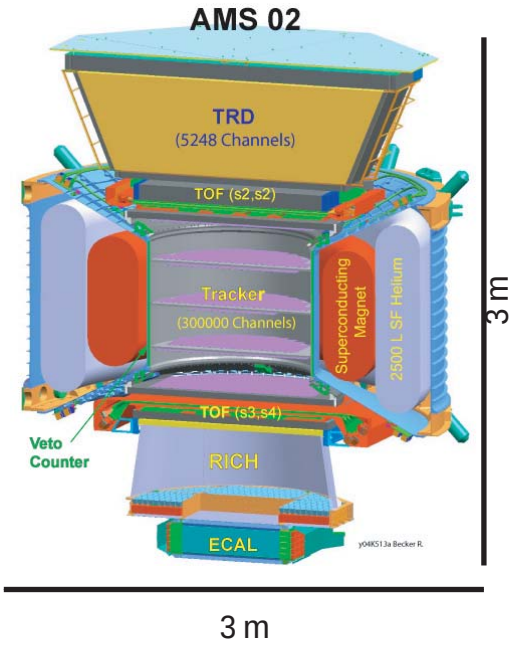

Figure 1. Schematic view of the AMS detector.

The calorimeter is an imaging calorimeter consisting of 9 modules of lead with embedded scintillating fibers corresponding in total to a thickness of 16.2 cm. Fibers are oriented along one or the other horizontal direction, alternatively for each module, as depicted in Figure 2, the incidence of the particles being vertical. The calorimeter has a sensitive surface of 648×648 mm^2.

Fibers are read at one end by 4-anodes photomultipliers (PMt :R7600-00-M4 Hamamatsu) giving an ultimate granularity of 72 anode-cells in the horizontal plane and 18 points longitudinally, each cell collecting the light on a surface of approximatively 9×9 mm^2. The four 30mm-long light guides, the PMt and the front-end electronics are inserted in magnetic shielding iron tubes which are maintained around the calorimeter by an aluminium structure.

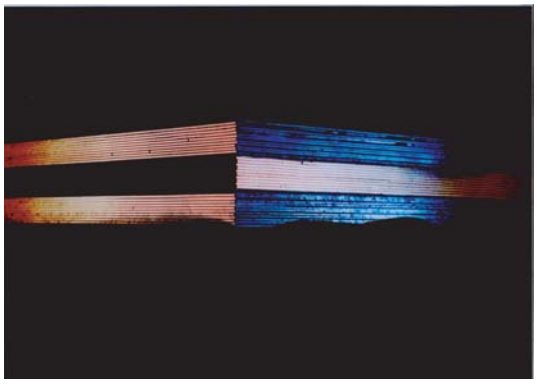

Figure 2. 3 modules of the calorimeter with enlightened fibers to illustrate the structure. There are 9 layers in total.

Figure 3. The calorimeter fully equipped with front-end electronics.

The flight model fully equipped with the frond-electronics is shown in Figure 3.

Dynamically, the expected signal from cosmic rays ranges from a few photoelectrons for Minimum ionizing Particles (non interacting protons) to about 10^5 for electromagnetic showers in the TeV range. To cope with this dynamic range, the front end electronics is designed with two gains and a ratio high to low of 33 on average.

3. Test-Beam setup

The flight model of the calorimeter was tested on a beam line of the CERN SPS accelerator ring in October 2006 and July 2007. Fully instrumented with the flight electronics, it was carefully wrapped in a plastic film to protect it from dust. It was fixed on a support structure which could move along X (horizontal) and Y (vertical) with respect to the beam direction (Z axis) and which could rotate around the vertical axis. With the test beam setup, 5 (resp. 4) layers were measuring the position and energy in X(Y). Electron beams of energies between 6 to 250 GeV and hadron beams with energy ranging from 20 to 100 GeV were used. Data were recorded essentially in the center of the calorimeter and scanning along the X and Y directions.

4. Slow Control

The calorimeter must be able to survive extreme temperatures without irreversible damages, the reference temperatures being -30 °C and + 50°C. Consequently, it should be able to operate for a wide range of temperature. During the test beam, thanks to sensors located close to the PMts' electronics on the aluminium back panel, the temperature was recorded in several points on each face and could then be extrapolated in each point. The pedestal dependance with respect to the temperature was studied and found compatible with the studies done in the laboratory. Figures 4 et 5 show respectively a map of the temperature and a typical pedestal dependance. With an average dependance of 0.45 ADC counts per degree, 3 channels out of 2592 have a 0 (negative) pedestal at -20°C.

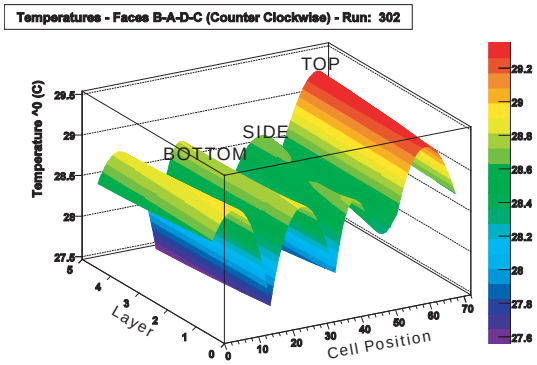

Figure 4. Map of the extrapolated temperatures on each face on the calorimeter.

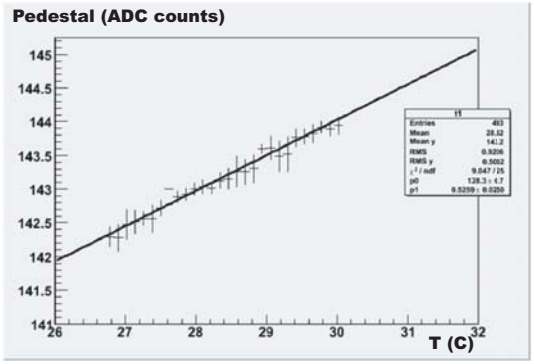

Figure 5. A typical dependence of the pedestal as a function of the temperature.

5. Energy reconstruction

Several corrections are applied to reconstruct the energy of electrons. They are detailed in the following subsections.

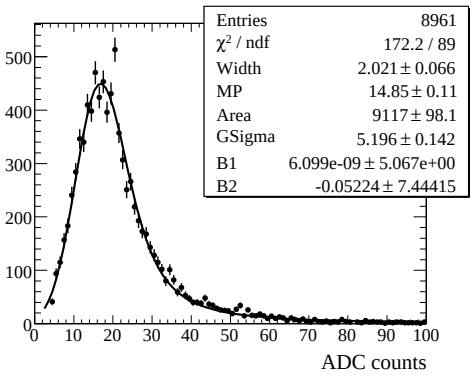

Figure 6. Example a MIP distribution fitted with a Landau convoluted by a Gaussian function + an exponential background,

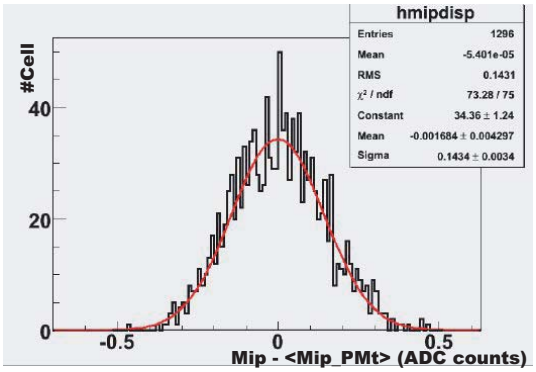

Figure 7. Dispersion of MIPs within PMts observed in test beam.

5.1. Equalization

The first set of corrections is meant to equalize the response of each anode and to treat the high to low gain ratio individually. The equalization is performed using the MIP signal obtained in each cell from a scan along the X and Y axis in the middle of the calorimeter by a 100 GeV hadron beam [1]. Each distribution is fitted by a Landau function convoluted by a Gaussian function plus an exponential background and an example is given in Figure 6. The MIPs were distributed with an average of 15 ADC counts and a sigma of 2.3 ADC counts. The dispersion within a PMt as shown in Figure 7, amounts to 15% in agreement with the specifications. Figure 8 displays an example of the correlation between high and low gain measurements. The distribution of gains measured in the test beam is shown in Figure 9.

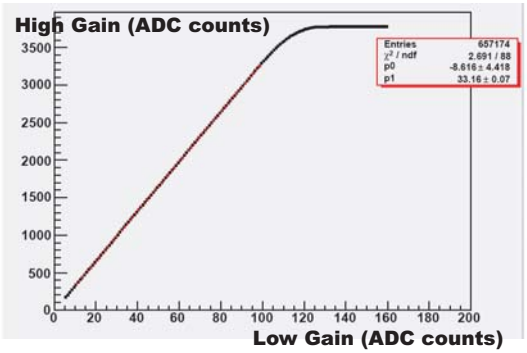

Figure 8. Relation between High to Low gain for a single anode.

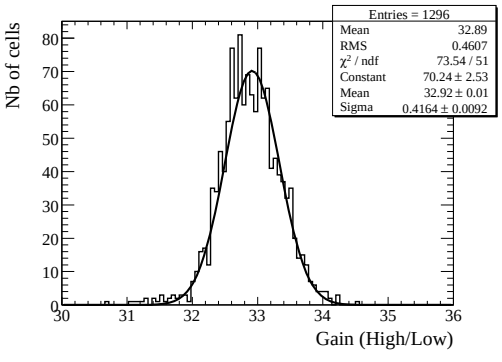

Figure 9. Distribution of the PMts' gains measured in test beam.

5.2. Attenuation

The signal is attenuated along the fibers and needs to be corrected depending upon the original position along the fibers. Scan along X and Y with electrons at 10 and 30 GeV and with hadrons

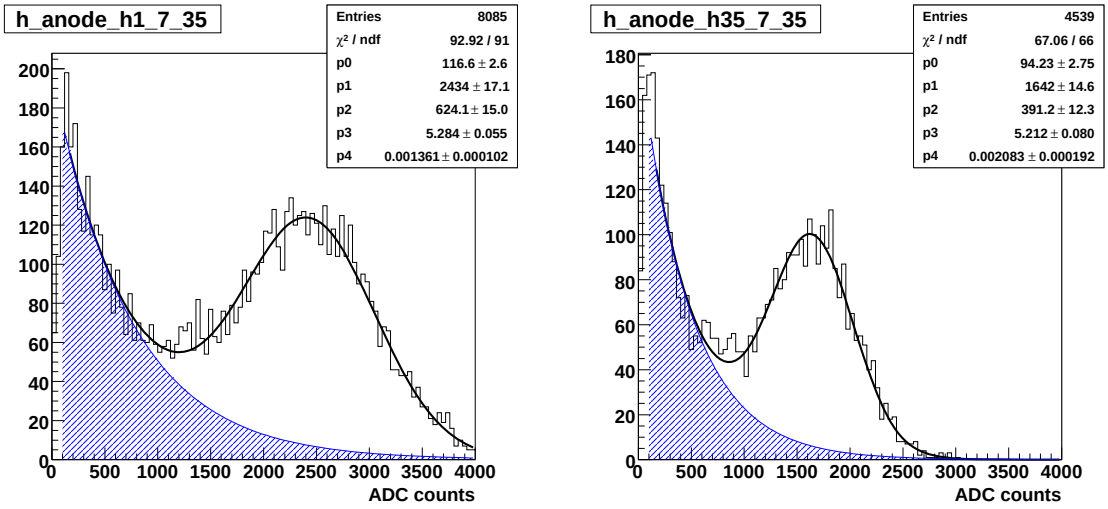

Figure 10. 10 GeV Electron signal measured close (left) and far (right) from the photomultiplier.

are used to measure the attenuation. An example of the signal of 10 GeV electrons recorded close and far from the PMt is shown in Figure 10. Similarly the MIP peak evolves along the fibers as shown in Figure 11. All attenuation curves are fitted simultaneously by the following function $f \times \exp(-x/\lambda_{fast}) + (1-f) \times \exp(-x/\lambda_{slow})$ letting free an individual amplitude per cell.

An example of the result of the fit is given in Figure 12. The correction is applied such that there is no correction in the center of the calorimeter: the effect of the correction on the energy measured in one layer is depicted in Figure 15.

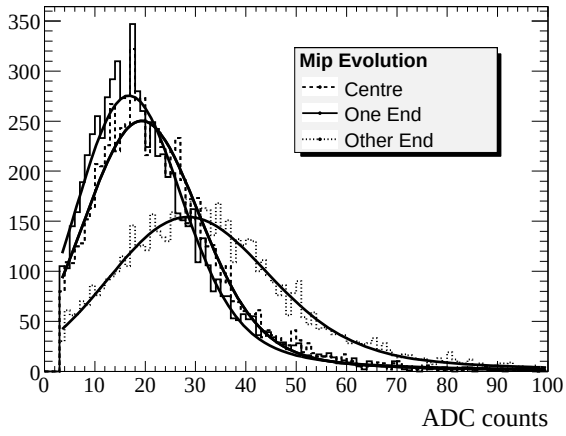

Figure 11. MIP signal measured at three different positions along the fiber.

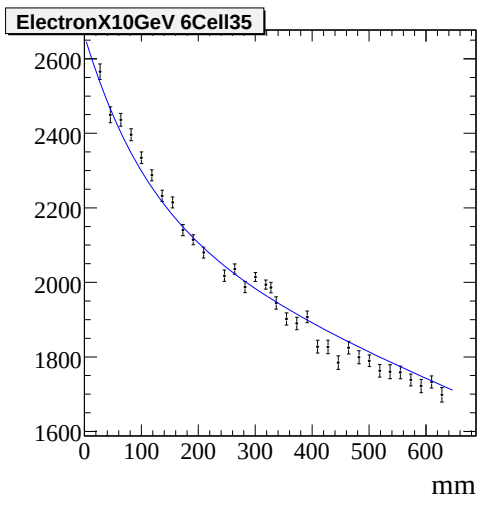

Figure 12. Example of fit of the attenuation.

5.3. Impact correction

The energy measurement is sensitive to the impact of the particle with respect to the boundaries of the cell as illustrated in Figure 13. To correct for this, a method adapted from [2] was used. It relies on the fact that the ratio S1/S3 of the energy in the cell with the maximum energy to the energy of the neighboring ones per layer and summed over all layers in one direction has a better sensitivity to the impact point (Figure 13). A simple dependance of this ratio to the energy can be observed as shown in Figure 14. The normalized inverse shape of this function is used to correct for the impact dependance and the result is given in Figure 16.

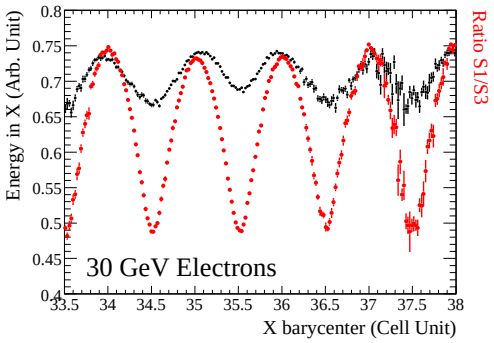

Figure 13. Sensitivity of the energy reconstruction to the impact position given by the barycenter (small black dots), Sensitivity of the ratio S1/S3 (See text) to the impact position (large red dots)

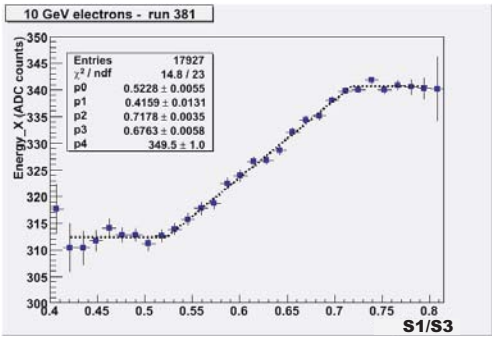

Figure 14. Dependance of the energy as a function of S1/S3 (See text).

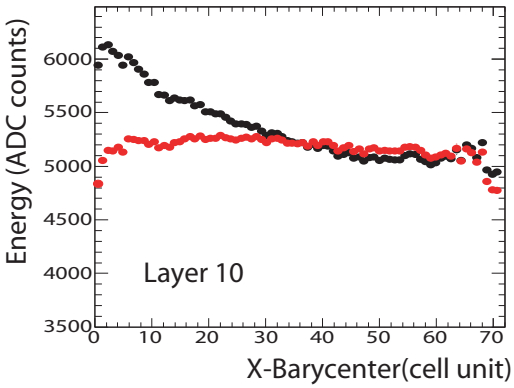

Figure 15. Energy measured in layer 10 before (black) and after (grey/red) correcting for the attenuation as a function of the X position.

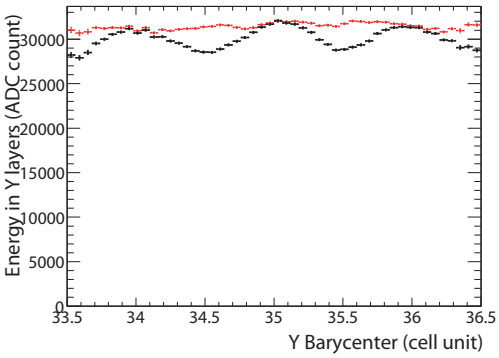

Figure 16. Energy before (black) and after (grey/red) impact correction.

5.4. Rear Leakage correction

The last correction will correct for the energy leakage. The relative leakage energy is approximated by a linear function of the fraction of energy measured in the latest layers of the calorimeter [3]. Figure 17 exemplifies this relation with 100 GeV electrons and in Figure 18,

it can be seen that the linear relation scales with the beam energy. Therefore this dependance was taken into account using the energy divided by the longitudinal barycenter which is roughly proportional to the incident energy . Figure 19 shows the reconstructed energy before and after leakage correction.

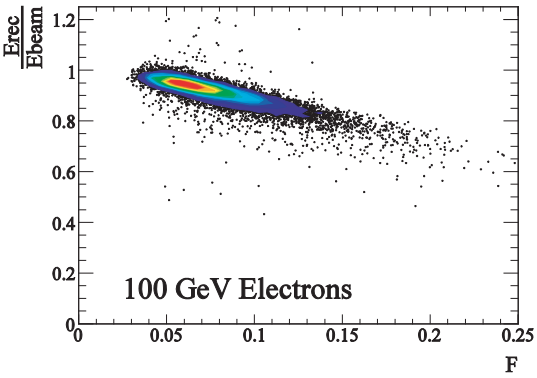

Figure 17. Example of the linear dependence of the relative leakage energy, given by the ratio of the reconstructed energy Erec, (including all preceding corrections) over the beam energy as a function of F, the fraction of energy in the last two layers for 100 GeV Electrons

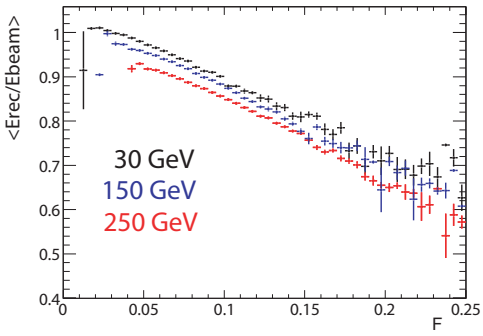

Figure 18. Average relative leakage energy as a function of the fraction of energy in the last two layers for 3 incident beam energies.

6. Performances

Preliminary results on the resolution and the linearity are shown in Figures 20 and 21. The resolution was fitted to be $\sigma/E = 10.3\%/\sqrt{E} \oplus 1.6\%$ while the linearity is kept within 2%. Using the same complete set of corrections, the linearity and the resolution are not degraded when the incidence angle of the beam is 15 degrees. Using the fit to the longitudinal profiles of all energies, displayed for 3 energies in Figures 22, the radiation length X_0 can be deduced: it was fitted to be 1.07(0.02) layer unit. Therefore, the calorimeter consists of 16.9 radiation lengths.

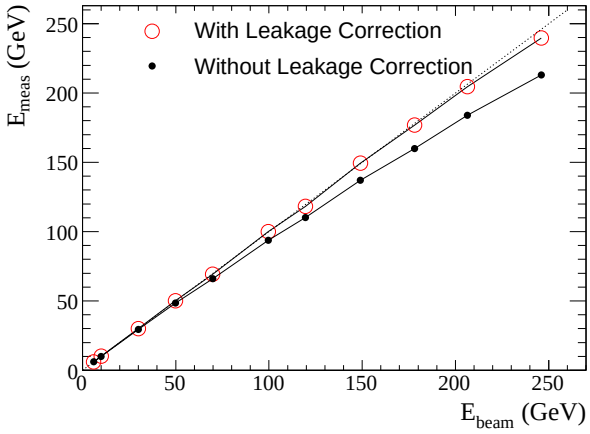

Figure 19. Energy before and after leakage correction in function of the beam energy.

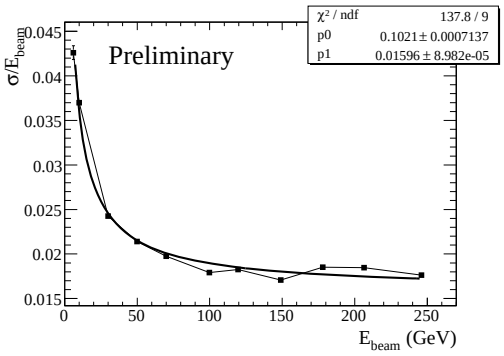

Figure 20. Preliminary results on the energy resolution.

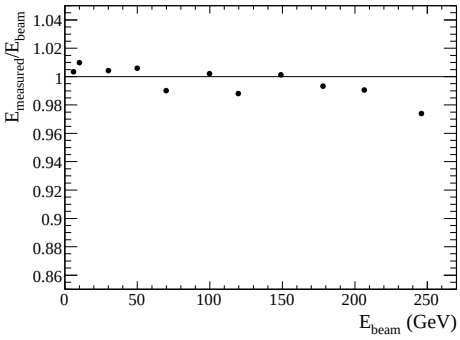

Figure 21. Preliminary result on the linearity.

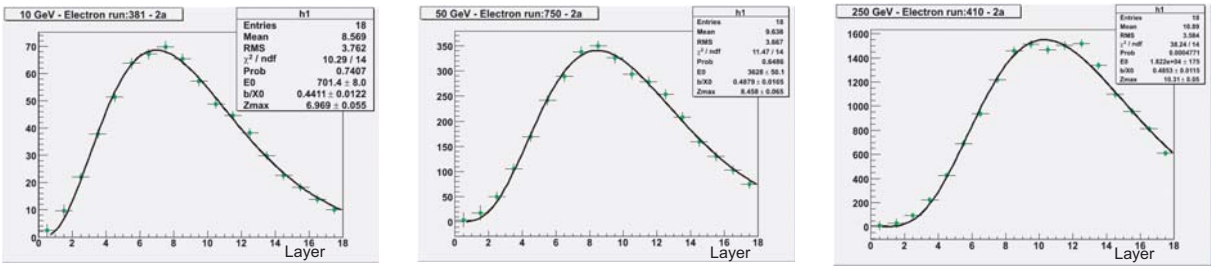

Figure 22. Longitudinal electromagnetic profiles fitted from left to right at the energies of 10, 50 and 250 GeV.

7. Conclusion

The beam tests of the flight model of the AMS calorimeter were successful. No channels were found dead or noisy. Preliminary results for the resolution and linearity are very encouraging: a constant term of 1.6% was obtained while the linearity is kept within 2% in the energy range from 6 to 250 GeV. Further refinements on the different corrections are expected to improve the constant term. The calorimeter was found to be 16.9 radiation lengths thick.

References

[1] AMS note 2008-01-01
[2] The L3 Collobration,*Nucl. Inst. Meth.* A **289**(1990) 35
L3 note 1712, (1995)
[3] Loic Girard. *PhD thesis*(2004) and reference therein.